

## Supplementary Information

### **Introducing Ionic and/or Hydrogen Bonds into the SAM//Ga<sub>2</sub>O<sub>3</sub> Top- Interface of Ag<sup>TS</sup>/S(CH<sub>2</sub>)<sub>n</sub>T//Ga<sub>2</sub>O<sub>3</sub>/EGaIn Junctions**

Carleen M. Bowers,<sup>1</sup> Kung-Ching Liao,<sup>1</sup> Hyo Jae Yoon,<sup>1</sup> Dmitrij Rappoport,<sup>1</sup> Mostafa Baghbanzadeh,<sup>1</sup> Felice C. Simeone,<sup>1</sup> and George M. Whitesides<sup>1,2\*</sup>

<sup>1</sup>Department of Chemistry and Chemical Biology, Harvard University,  
12 Oxford Street, Cambridge, Massachusetts 02138 United States,

<sup>2</sup>Kavli Institute for Bionano Science & Technology, Harvard University,  
29 Oxford Street, Massachusetts 02138 United States

\*Corresponding author, email: [gwhitesides@gmwgroup.harvard.edu](mailto:gwhitesides@gmwgroup.harvard.edu)

## Experimental Details

**Materials.** Precursors to all monolayers (with the exception of HS(CH<sub>2</sub>)<sub>5</sub>CONH<sub>2</sub>) were commercially available ( $\geq 98\%$ , Sigma-Aldrich). All organic solvents were analytical grade (99%, Sigma-Aldrich) and were used as supplied unless otherwise specified. The synthesis of HS(CH<sub>2</sub>)<sub>5</sub>CONH<sub>2</sub> is described below. All thiolate-based compounds were maintained under a N<sub>2</sub> atmosphere at  $< 4^\circ\text{C}$  to avoid oxidation to the corresponding disulfide, sulfonate, or sulfonic acid. To ensure that the compounds were free of contaminants, all stored compounds were checked by <sup>1</sup>H NMR prior to use. Impurities were carefully removed by silica gel column chromatography (100% hexane). All organic solvents were analytical grade (99%, Sigma-Aldrich) and were used as supplied unless otherwise specified.

**The EGaIn Technique.** EGaIn (eutectic Ga-In; 74.5% Ga, 25.5% In) has emerged as a convenient and attractive material for forming top-contacts and measuring currents in junction devices having the structure Ag<sup>TS</sup>/SAM//Ga<sub>2</sub>O<sub>3</sub>/EGaIn.<sup>1</sup> As a liquid metal with a self-passivating oxide layer of Ga<sub>2</sub>O<sub>3</sub> (0.7 nm thick on average),<sup>2</sup> this technique offers the advantage of forming non-damaging top contacts and results in high yields ( $>90\%$ ) of working (non-shortening) junctions. Moreover, the apparent non-Newtonian behavior of EGaIn (a reflection of the mechanical properties of the electrically conducting Ga<sub>2</sub>O<sub>3</sub> film that forms on its surface) facilitates the formation of sharp conical tips (enabling a small geometrical contact area of  $\sim 25\ \mu\text{m}$  in diameter, or  $\sim 490\ \mu\text{m}^2$  in geometrical contact area estimated by microscopy). Understanding the influence of the SAM-metal oxide interface on charge tunneling is the focus of this particular investigation.

**Selected Conical Tips.** We selected EGaIn conical tips that were free of visible surface

asperities (Figure S1b). Conical tips that had visible irregularities (as seen by optical microscopy) were discarded (Figure S1a).

**Template-Stripped Silver ( $\text{Ag}^{\text{TS}}$ ) Bottom Electrode.** We formed SAMs on template-stripped silver substrates ( $\text{Ag}^{\text{TS}}$ ). “Template stripping” provides a relatively flat surface compared to “as-deposited” (by an electron beam evaporator, rms roughness = 1.2 nm *vs.* 5.1 nm, over a  $25 \mu\text{m}^2$  area of Ag).<sup>3</sup> SAMs formed on the surfaces of  $\text{Ag}^{\text{TS}}$  have less defects than SAMs on as-deposited surfaces, and result in junction measurements with higher yields and with smaller dispersions in  $J(V)$  than as-deposited bottom electrodes.<sup>4,5</sup> Exact details of preparation of films, and of their characterization, are described elsewhere.<sup>3</sup>

**Preparation of Monolayers.** We followed previously published protocols for the formation of SAMs on  $\text{Ag}^{\text{TS}}$ .<sup>6-10</sup> Briefly,  $\text{Ag}^{\text{TS}}$  were submerged in a 3-mM ethanolic solution of thiolate for 16-18 hours at room temperature and under a nitrogen atmosphere. We rinsed the SAM-bound substrates with filtered ethanol, and dried them under a gentle stream of nitrogen.

***n*-Alkanethiolates as Standards.** Simple *n*-alkanethiolates served as internal standards for this work, and ensured that the apparatus and the operators were reproducing previous values of current densities. Junctions of the structure  $\text{Ag}^{\text{TS}}/\text{S}(\text{CH}_2)_n\text{CH}_3//\text{Ga}_2\text{O}_3/\text{EGaIn}$  are, by now, well-characterized and increasingly well-understood,<sup>11</sup> and the values of both  $J_0$  and  $\beta$  for *n*-alkanethiolates are available for a variety of large-area and single-molecule junctions.<sup>12</sup>

**SAMs Bearing Terminal  $\text{CO}_2\text{H}$  groups.** Nuzzo *et al.* proposed that approximately 50% of neighboring  $\text{CO}_2\text{H}$  groups at the terminus of a SAM form linear chains of hydrogen bonds.<sup>13</sup> SAMs terminated in  $\text{CO}_2\text{H}$  groups are also capable of hydrogen bonding through lone pairs of electrons on one of both of the oxygen atoms.<sup>14, 15</sup>

To ensure that the thiolate group binds preferentially to the Ag<sup>TS</sup> substrate, and leaves the carboxylic acid exposed at the interface with Ga<sub>2</sub>O<sub>3</sub>, we measured stationary contact angles ( $\theta_s$ ) of water on the surface of these SAMs. The values of  $\theta_s$  ( $\sim 20^\circ$  for HSC<sub>7</sub>CO<sub>2</sub>H on Ag<sup>TS</sup>) were consistent with literature values<sup>16</sup> and indicate that the polar protic –CO<sub>2</sub>H group is exposed at the surface of the SAM (Table S2 summarizes the values of  $\theta_s$ ). We also characterized the SAMs with X-ray photoelectron spectroscopy (XPS; Thermo Scientific K-Alpha photoelectron spectrometer with Monochromatic Al K- $\alpha$  X-ray radiation (1.49 kV at base pressure  $\sim 10^{-9}$  Torr)). All spectra show the presence of sulfur (S 2p<sub>3/2</sub> and S p<sub>1/2</sub>) with binding energies ( $\sim 163$  and 162 eV) consistent with sulfur bound to silver (Figure S3).<sup>17</sup>

**Electrical Measurement Protocol.** We formed SAMs on Ag<sup>TS</sup> and used “unflattened”<sup>11</sup> conical tips of Ga<sub>2</sub>O<sub>3</sub>/EGaIn to fabricate Ag<sup>TS</sup>/S(CH<sub>2</sub>)<sub>n</sub>T//Ga<sub>2</sub>O<sub>3</sub>/EGaIn junctions.<sup>3</sup> Although we did not cycle the voltage ( $\pm 1$  V) across the conical tips while in contact with a silicon substrate,<sup>11</sup> the tips we used to measure were free of visible asperities (Figure S1). Furthermore, the values of current density measured using “flattened” and “unflattened” conical tips are indistinguishable. We measured charge-transport across the SAMs at  $\pm 0.5$  V by sweeping in both directions starting at 0 V (i.e. one sweep 0 V  $\rightarrow$  +0.5 V  $\rightarrow$  0 V  $\rightarrow$  0.5 V  $\rightarrow$  0 V, in steps of 0.05 V).

**Influence of Humidity on the Rate of Charge Transport.** In a separate investigation,<sup>18</sup> we have demonstrated that different levels of relative humidity (from 20 to 60% RH) in the environment in which charge transport is measured do not affect the rates of charge transport. Specifically, increasing the relative humidity does not result in changes in current density for methyl-terminated or carboxyl-terminated *n*-alkanethiolates on Ag<sup>TS</sup>. Therefore, the components of the junction (namely the EGaIn electrode and the SAM) are not susceptible to changes in resistance upon exposure to increasing humidity. Moreover, the measurements reported here

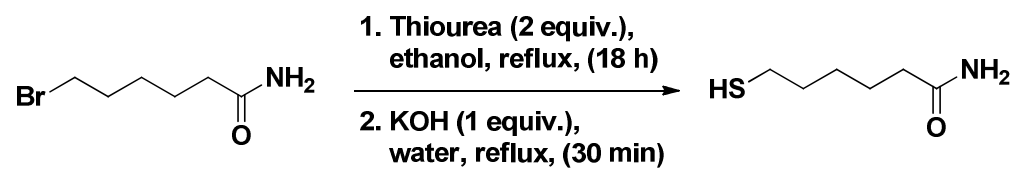
were obtained under similar laboratory environments ( $25\% < \text{RH} < 35\%$ ), so we do not anticipate the humidity to affect the current density measurements of either the Lewis acid/base terminated SAMs or the standards.

**Rectification.** We measured  $J(V)$  for junctions of the form  $\text{Ag}^{\text{TS}}/\text{S}(\text{CH}_2)_n\text{CO}_2\text{H}/\text{Ga}_2\text{O}_3/\text{EGaIn}$  over a voltage range of  $\pm 0.5$  V, where  $n = 3, 5, 7, 11, 15$ ; we did not observe rectification of current (Figure S4).

**DFT Computational Details.** The electronic structure of the alkanethiolates and carboxylic acid terminated alkanethiolates were modeled by small-cluster models using the  $\text{Ag}_9$  cluster. The calculations of orbital energies were performed with density functional theory (DFT) using the Becke hybrid functional B3-LYP<sup>19</sup> and resolution-of-the-identity approximation for the Coulomb energy (RI-J);<sup>20</sup> def2-SVP Gaussian basis sets<sup>21</sup> were used along with corresponding auxiliary basis sets<sup>22</sup> and small-core relativistic effective core potentials (ECPs) for Ag.<sup>23</sup> All calculations were carried out within the Turbomole suite of programs (V6.4, 2012).

**Synthesis of  $\text{HS}(\text{CH}_2)_5\text{CONH}_2$ :** A 25 mL ethanolic solution containing  $\text{Br}(\text{CH}_2)_5\text{CONH}_2$  (965 mg, 4 mmol) and thiourea (608 mg, 8 mmol) was heated under reflux for 18 hrs. After being cooled to room temperature, the reaction solvent was removed *in vacuo*, followed by the addition of an aqueous solution of KOH (246 mg, 4.4 mmol in 20 mL degassed water). The reaction mixture was again heated under reflux for 30 min under  $\text{N}_2$  atmosphere (Note: longer reaction times may result in oxidation of the thiol group). The reaction solution was cooled to room temperature and extracted with cold  $\text{CH}_2\text{Cl}_2$ . The combined organic layer was dried over anhydrous  $\text{MgSO}_4$ , filtered to remove the suspended solid, and concentrated *in vacuo* (Note: the temperature of water bath must be below  $30^\circ\text{C}$ ) to yield the title compound.  $^1\text{H}$  NMR ( $\text{CDCl}_3$ ):  $\delta$

5.56 (brs, 2H,  $NH_2$ ), 2.51 (q,  $J = 7.2$  Hz, 2H), 2.21 (t,  $J = 7.2$  Hz, 2H), 1.68 – 1.57 (m, 4H), 1.46 – 1.40 (m, 2H), 1.33 (t,  $J = 7.6$  Hz, 1H, *SH*).  $^{13}C\{^1H\}$  NMR ( $CDCl_3$ ):  $\delta$  175.4, 35.6, 33.6, 27.8, 24.8, 24.4. HRMS ( $m/z$ ) calcd. for  $[C_6H_{13}NOS]^+$  ( $M+H^+$ ): 148.0796; found: 148.0782.



**Scheme S1.** Synthetic scheme for the preparation of  $\text{HS}(\text{CH}_2)_5\text{CONH}_2$

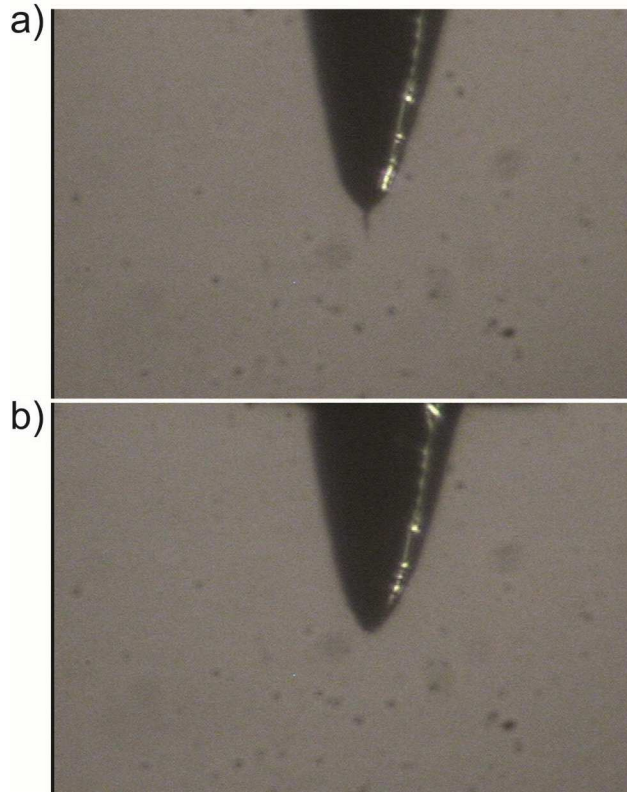


**Figure S1.** Photographs of fabricated conical tips. (a) An example of a conical tip containing surface asperities (here a “whisker”); this type of tip would be discarded. (b) An example of a conical tip that is free of visible surface asperities; this tip would be appropriate to use for the collection of  $J(V)$  scans.

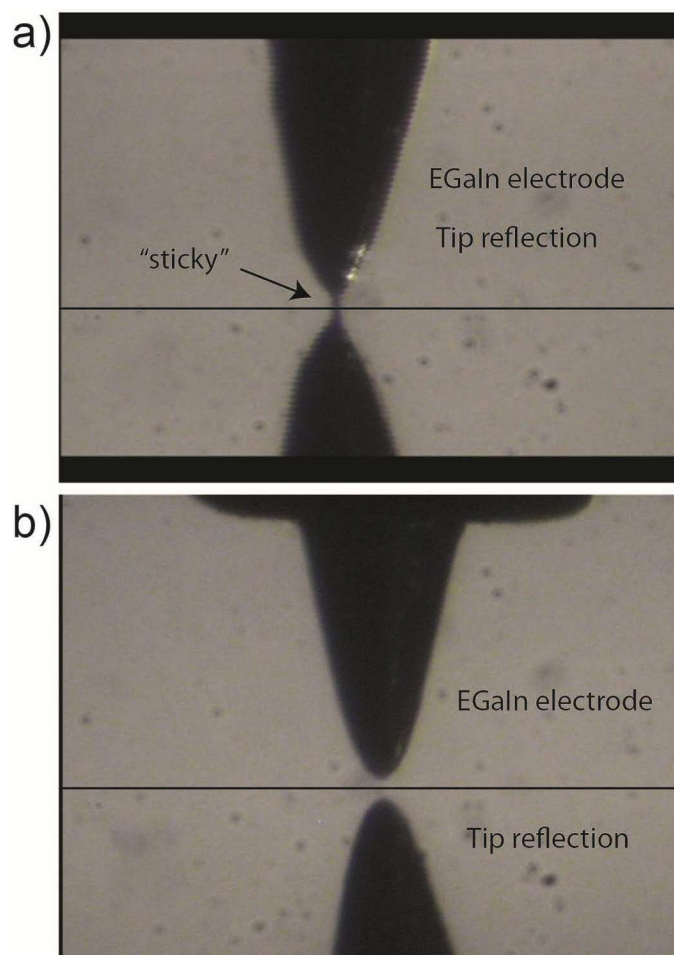


**Figure S2.** a) Photograph depicting the adhesion of the EGaIn top electrode with a CO<sub>2</sub>H terminated alkanethiolate (SC<sub>7</sub>CO<sub>2</sub>H) SAM on Ag<sup>TS</sup>. b) An example of the typical “non-sticky” interaction between EGaIn and a methyl-terminated alkanethiolate (S(CH<sub>2</sub>)<sub>n</sub>CH<sub>3</sub> on Ag<sup>TS</sup>).

**Table S1.** Summary of static water-wetting contact angles ( $\theta_s$ ) for CO<sub>2</sub>H terminated alkanethiolates on Ag<sup>TS</sup> and advancing ( $\theta_a$ ) and receding water contact angle ( $\theta_r$ ) for *n*-alkanethiolates on Ag. The advancing ( $\theta_a$ ) and receding contact angle ( $\theta_r$ ) data for *n*-alkanethiolates were taken from reference 9.

SAM on Ag <sup>TS</sup>	mean contact angle ( $\theta_s$ ) and standard deviation	SAM on Ag	contact angle ( $\theta_a, \theta_r$ ) <sup>17</sup>
SC <sub>3</sub> CO <sub>2</sub> H	17 ± 2	S(CH <sub>2</sub> ) <sub>3</sub> CH <sub>3</sub>	~100, ~ 90
SC <sub>5</sub> CO <sub>2</sub> H	21 ± 2	S(CH <sub>2</sub> ) <sub>5</sub> CH <sub>3</sub>	~108, ~ 95
SC <sub>7</sub> CO <sub>2</sub> H	21 ± 1	S(CH <sub>2</sub> ) <sub>7</sub> CH <sub>3</sub>	~110, ~ 100
SC <sub>11</sub> CO <sub>2</sub> H	24 ± 1	S(CH <sub>2</sub> ) <sub>10</sub> CH <sub>3</sub>	~110, ~ 100
SC <sub>15</sub> CO <sub>2</sub> H	33 ± 2	S(CH <sub>2</sub> ) <sub>15</sub> CH <sub>3</sub>	~110, ~ 102

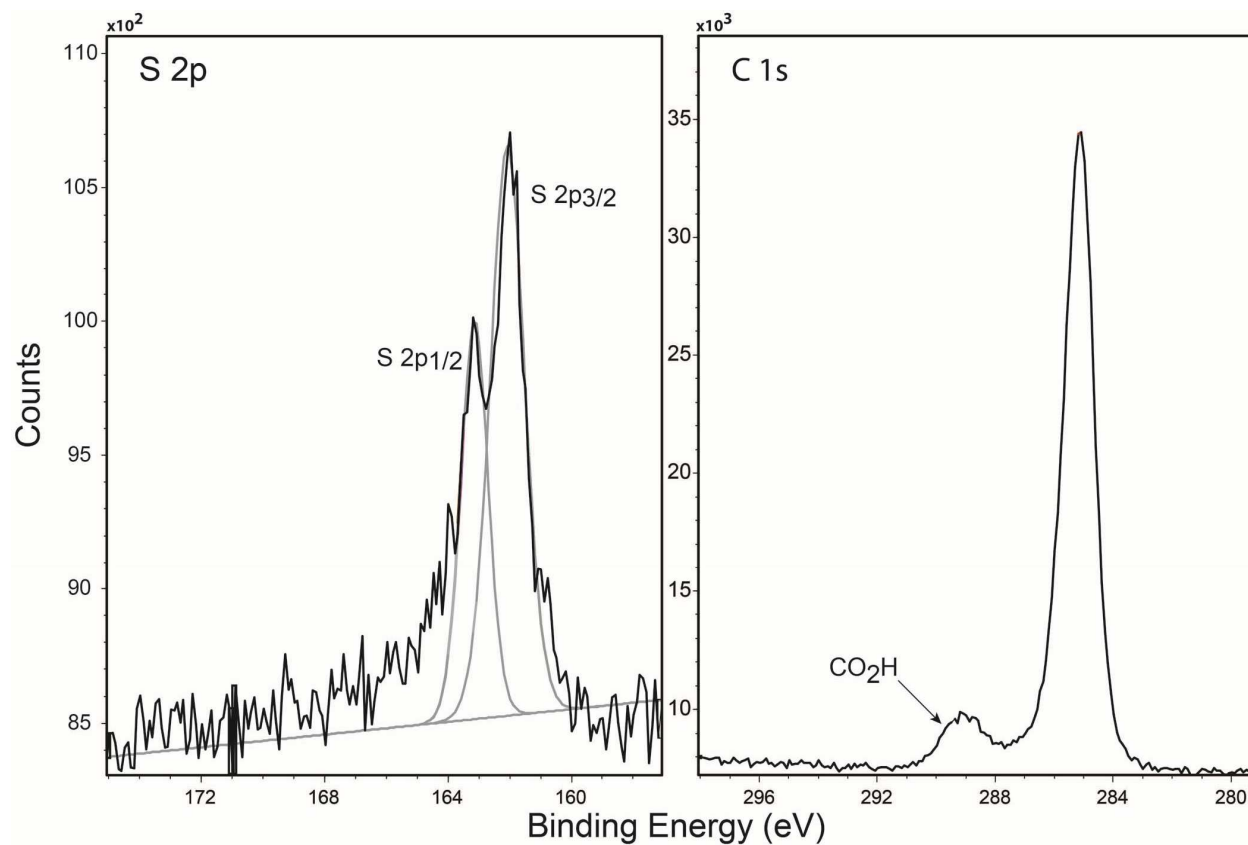


**Figure S3.** XPS spectra of S 2p and C 1s regions from a SAM of 12-mercaptododecanoic acid on Ag.<sup>TS</sup> The two peaks present for S 2p arise from the orbital doublet S 2p<sub>3/2</sub> (~ 162 eV) and S 2p<sub>1/2</sub> (~163 eV).

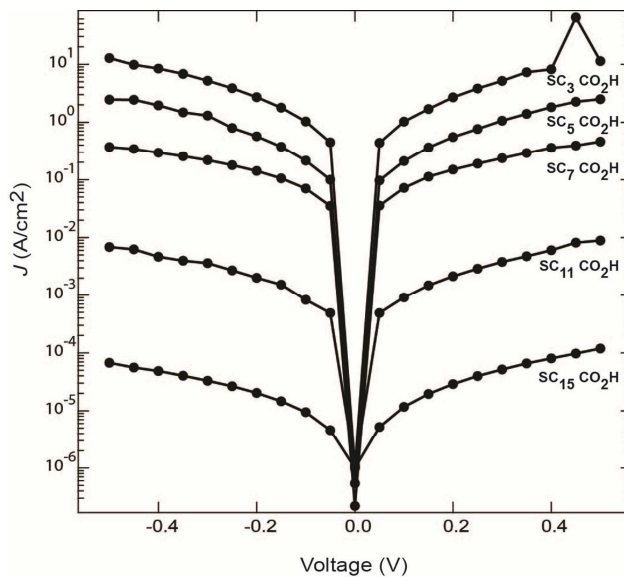


**Figure S4.** A plot of current density ( $J$ ) versus bias ( $V$ ) for the  $\text{Ag}^{\text{TS}}/\text{S}(\text{CH}_2)_n\text{CO}_2\text{H}/\text{Ga}_2\text{O}_3/\text{EGaIn}$  junctions with various chain lengths ( $n= 3, 5, 7, 11, 15$ ), as indicated in the Figure. We did not observe rectification of current.

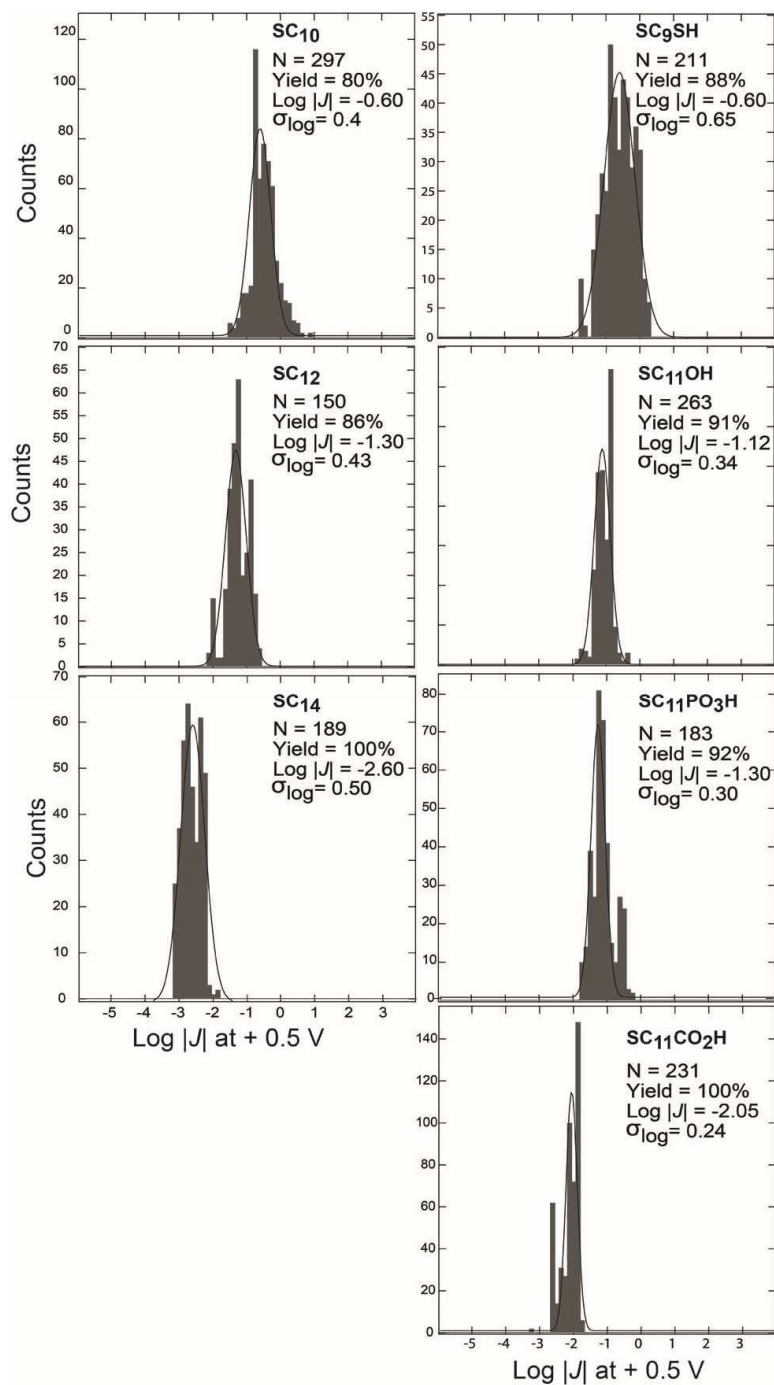


**Figure S5.** Histograms of  $\log|J|$  at +0.5 V across  $\text{Ag}^{\text{TS}}\text{SAM}/\text{Ga}_2\text{O}_3/\text{EGaIn}$  junctions using conical tips. Solid curves represent Gaussian fits;  $N$  is the number of data points. The  $n$ -alkanethiolate (SC<sub>10</sub>, SC<sub>12</sub>, and SC<sub>14</sub>) serve as an internal standard; having a similar number of atoms to the thiolates bearing terminal functional groups

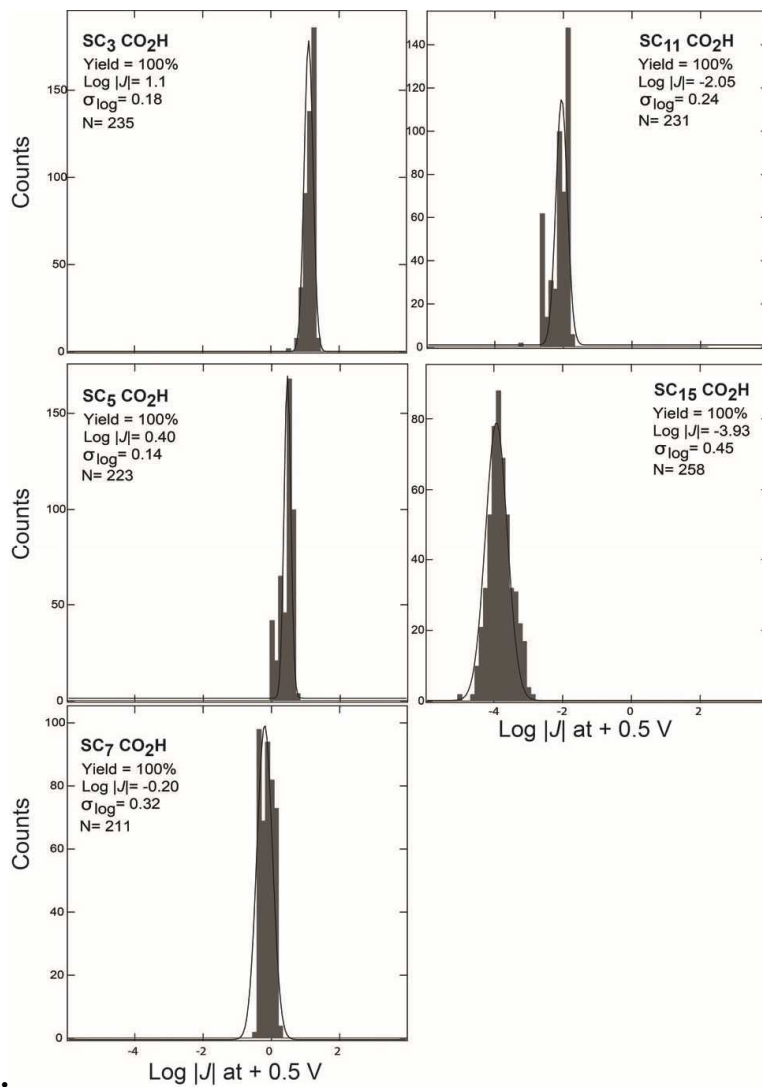


**Figure S6.** Histograms of  $\log|J|$  at +0.5 V for carboxylic acid-terminated alkanethiolates across  $\text{Ag}^{\text{TS}}/\text{S}(\text{CH}_2)_n\text{T}/\text{Ga}_2\text{O}_3/\text{EGaIn}$  junctions using “unflattened” conical tips. Solid curves indicate a Gaussian fit and N indicates the number of data points

**Table SII.** Calculated energies for HOMO and LUMO of *n*-alkanethiolates and  $\omega$ -carboxyl-alkanethiolates on silver clusters using density functional theory (DFT).<sup>19-23</sup>

SAM on Ag	HOMO (eV)	LUMO (eV)	SAM on Ag	HOMO (eV)	LUMO (eV)
SC <sub>1</sub> CH <sub>3</sub>	-4.89	-2.92	SC <sub>1</sub> CO <sub>2</sub> H	-5.17	-3.07
SC <sub>3</sub> CH <sub>3</sub>	-4.89	-2.92	SC <sub>3</sub> CO <sub>2</sub> H	-5.02	-3.00
SC <sub>6</sub> CH <sub>3</sub>	-4.89	-2.92	SC <sub>5</sub> CO <sub>2</sub> H	-4.97	-2.97
SC <sub>7</sub> CH <sub>3</sub>	-4.89	-2.92	SC <sub>8</sub> CO <sub>2</sub> H	-4.94	-2.95
SC <sub>9</sub> CH <sub>3</sub>	-4.89	-2.92	SC <sub>9</sub> CO <sub>2</sub> H	-4.93	-2.94
SC <sub>11</sub> CH <sub>3</sub>	-4.89	-2.92	SC <sub>11</sub> CO <sub>2</sub> H	-4.90	-2.93
SC <sub>13</sub> CH <sub>3</sub>	-4.89	-2.92	SC <sub>13</sub> CO <sub>2</sub> H	-4.91	-2.93
SC <sub>15</sub> CH <sub>3</sub>	-4.89	-2.92	SC <sub>15</sub> CO <sub>2</sub> H	-4.91	-2.93

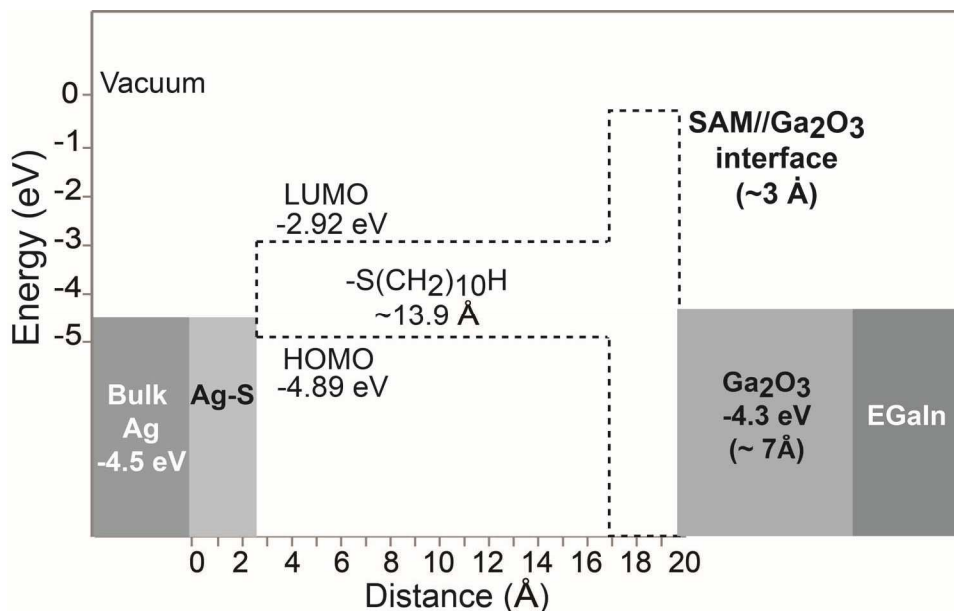


**Figure S7.** Schematic description of some characteristics of the tunneling barrier (with respect to vacuum) of the  $Ag^{TS}/S(CH_2)_nH/Ga_2O_3/EGaIn$  junction (here,  $n = 10$ ) at zero applied bias. The work functions of Ag ( $\sim -4.5$  eV) and EGaIn ( $\sim -4.2$  eV) have been reported in the literature.<sup>24, 25</sup> DFT calculations were used to estimate the values of the frontier orbital energies—highest occupied molecular orbital, HOMO ( $-4.89$  eV), and lowest unoccupied molecular orbital, LUMO ( $-2.92$  eV)—for a cluster of  $n$ -decanethiolate ( $SC_{10}$ ) bound to Ag. The van der Waals contact distance of  $3 \text{ \AA}$  is an estimation from the van der Waals radius of the terminal hydrogen atom of the SAM and the oxygen atom of the  $Ga_2O_3$  film.

## References

1. Chiechi, R. C.; Weiss, E. A.; Dickey, M. D.; Whitesides, G. M. *Angew. Chem., Int. Ed.* **2008**, *47*, 142-144.
2. Cademartiri, L.; Thuo, M. M.; Nijhuis, C. A.; Reus, W. F.; Tricard, S.; Barber, J. R.; Sodhi, R. N. S.; Brodersen, P.; Kim, C.; Chiechi, R. C.; Whitesides, G. M. *J. Phys. Chem. C* **2012**, *116*, 10848-10860.
3. Weiss, E. A.; Kaufman, G. K.; Kriebel, J. K.; Li, Z.; Schalek, R.; Whitesides, G. M. *Langmuir* **2007**, *23*, 9686-9694.
4. Weiss, E. A.; Chiechi, R. C.; Kaufman, G. K.; Kriebel, J. K.; Li, Z. F.; Duati, M.; Rampi, M. A.; Whitesides, G. M. *J. Am. Chem. Soc.* **2007**, *129*, 4336-4349.
5. Yuan, L.; Jiang, L.; Zhang, B.; Nijhuis, C. A. *Angew. Chem. Int. Ed.* **2014**, *53*, 3377 – 3381.
6. Ulman, A. *Chem. Rev.* **1996**, *96*, 1533-1554.
7. Drelich, J.; Wilbur, J. L.; Miller, J. D.; Whitesides, G. M. *Langmuir* **1996**, *12*, 1913-1922.
8. Laibinis, P. E.; Bain, C. D.; Nuzzo, R. G.; Whitesides, G. M. *J. Phys. Chem.* **1995**, *99*, 7663-7676.
9. Bain, C. D.; Evall, J.; Whitesides, G. M. *J. Am. Chem. Soc.* **1989**, *111*, 7155-7164.
10. Bain, C. D.; Whitesides, G. M. *J. Am. Chem. Soc.* **1989**, *111*, 7164-7175.
11. Simeone, F. C.; Yoon, H. J.; Thuo, M. M.; Barber, J. R.; Smith, B.; Whitesides, G. M. *J. Am. Chem. Soc.* **2013**, *135*, 18131-18144.
12. McCreery, R. L.; Bergren, A. J. *Adv. Mat.* **2009**, *21*, 4303-4322.
13. Nuzzo, R. G.; Dubois, L. H.; Allara, D. L. *J. Am. Chem. Soc.* **1990**, *112*, 558-569.
14. Sun, L.; Crooks, R. M.; Ricco, A. J. *Langmuir* **1993**, *9*, 1775-1780.
15. Yang, H. C.; Dermody, D. L.; Xu, C. J.; Ricco, A. J.; Crooks, R. M. *Langmuir* **1996**, *12*, 726-735.
16. Bain, C. D.; Whitesides, G. M. *Langmuir* **1989**, *5*, 1370-1378.
17. Laibinis, P. E.; Whitesides, G. M.; Allara, D. L.; Tao, Y. T.; Parikh, A. N.; Nuzzo, R. G. *J. Am. Chem. Soc.* **1991**, *113*, 7152-7167.
18. Barber, J. R.; Yoon, H.J.; Thuo, M. M.; Bowers, C. M.; Breiten, B.; Gooding, D. M.; Whitesides, G. M. *Unpublished*.
19. Becke, A. D. *J. Chem. Phys.* **1993**, *98*, 5648-5652.

20. Eichkorn, K.; Treutler, O.; Ohm, H.; Haser, M.; Ahlrichs, R. *Chem. Phys. Lett.* **1995**, *242*, 652-660.
21. Weigend, F.; Ahlrichs, R. *Phys. Chem. Chem. Phys.* **2005**, *7*, 3297-3305.
22. Weigend, F. *Phys. Chem. Chem. Phys.* **2006**, *8*, 1057-1065.
23. Andrae, D.; Haussermann, U.; Dolg, M.; Stoll, H.; Preuss, H. *Theor. Chim. Acta* **1990**, *77*, 123-141.
24. Reus, W. F.; Thuo, M. M.; Shapiro, N. D.; Nijhuis, C. A.; Whitesides, G. M. *Acs Nano* **2012**, *6*, 4806-4822.
25. Chelvayohan, M.; Mee, C. H. B. *J. Phys. Chem. C* **1982**, *15*, 2305-2312.